PROCEEDINGS, Thirty-Seventh Workshop on Geothermal Reservoir Engineering
Stanford University, Stanford, California, January 30 - February 1, 2012
SGP-TR-194

GEOTHERMAL FIELD TESTS WITH FORCED GROUNDWATER FLOW

Dipl.-Ing. Heiko Huber & Prof. Dr.-Ing. Ulvi Arslan

Institute of Materials and Mechanics in Civil Engineering, Technical University Darmstadt
Petersenstraße 12
64287 Darmstadt, Germany
e-mail: huber@iwmb.tu-darmstadt.de

ABSTRACT

Currently our institute is performing a research program supported by the Federal Ministry of Economics and Technology (BMWi). The main objective of this research program is titled "experimental investigation for the verification of a Finite-Element-Multiphase-Model for heat transport processes in the ground" whereby the subsoil is analyzed as a three-phases-model with separate consideration of conduction, convection and their subsequent interaction.

Therefore, extensive experimental field tests are presently conducted at the Technical University Darmstadt (TUD). Geothermal Response Tests (GRT) as well as Enhanced Geothermal Response Tests (EGRT) are performed in different geological and hydrogeological conditions on two field test sites in Germany. With the help of pumping wells, unequal surrounding hydraulic heads are set to borehole heat exchangers in order to investigate the performance of GRTs and EGRTs depending on the forced groundwater flow. The groundwater flow is determined by the Groundwater Flow Visualization (GFV) measurement technique. As a result, groundwater flow velocities over borehole depth $v_f(z)$ were determined. The increase of the effective thermal conductivity over depth $\lambda_{eff}(z)$ is correlated with the determined groundwater flow velocities $v_f(z)$. The ratio of conductive to convective energy transport has been investigated. All results of field tests with different forced groundwater flows are compared to each other.

INTRODUCTION

For the design of smaller geothermal systems the geothermal, geological and hydrogeological parameters can be estimated according to common literature. For the design of complex geothermal systems the subsoil has to be modeled with numerical approaches based on the Finite-Element-Method (FEM) or the Finite-Difference-Method (FDM) using values evaluated in laboratory or *in-situ*. In saturated soils, especially in areas of groundwater flow, the energy transport of the fluid phase (convection) and the solid phase (conduction) as well as their interaction has to be considered separately for a proper numerical modeling of geothermal systems. Even in the case of low groundwater flow velocity of about 10^{-7} m s^{-1}, the role of convective heat transport cannot be neglected, (Katsura et al., 2009), (Spitler et al., 1999), (Kleiner, 2003), (Pannike et al., 2006).

Insofar, the available monitored data of the ratio of heat energy transported by convection to the entire transported heat energy in dependence of the groundwater flow velocity is insufficient (Glück, 2008). In order to optimize the modeling of geothermal systems a sufficient database of geothermal systems influenced by groundwater flow is essential. By means of this database numerical modeling programs for geothermal purpose can be verified.

Common tools for the determination of geothermal parameters *in-situ* are Geothermal Response Tests (GRT) and Enhanced Geothermal Response Tests (EGRT). While executing a GRT, the time dependent mean temperature increase of the fluid is monitored and the integral effective thermal conductivity of the whole BHE length λ_{eff} can be evaluated. However, the effective thermal conductivity of the enclosing ground varies in correlation with the geological and hydrogeological conditions over depths. Therefore, it is most important to get an idea of the diversity of the effective thermal conductivity over the BHE depth $\lambda_{eff}(z)$. To evaluate $\lambda_{eff}(z)$ the increasing temperature k over time must be determined for all the incremental depths of the borehole. This can be performed by the Distributed fibre optic Temperature Sensing (DTS) technique, which is used by EGRTs.

The theoretical background of EGRTs is described in (Hartog & Payne, 1982) and (Hurtig et al., 1993).

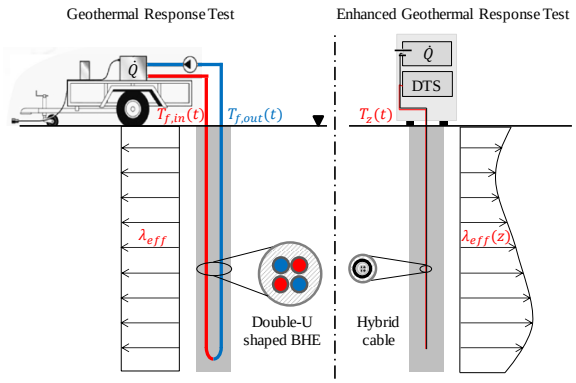

Figure 1. Schematic comparison of GRTs and EGRTs

Due to EGRTs, a hybrid cable consisting of fibre optic cable and copper wire is installed to a borehole or Borehole Heat Exchanger (BHE). A constant thermal load $\dot{Q}$ [W m^{-1}] is fed in the copper wire. The increase of temperature is measured over the fibre optic cable via Optic Time-Domain Reflectometry (OTDR) in every incremental depth of the borehole. $\lambda_{eff}(z)$ can be evaluated via the Source Theory. A schematic comparison of GRTs and EGRTs is illustrated in Fig. 1.

Witte & van Gelder [8] investigated the influence of groundwater flow velocities on the effective thermal conductivity λ_{eff} of GRTs. With a long-term pumping test at a neighbored pumping well an artificial hydraulic gradient was applied.

The resulting groundwater flow of 3 m d^{-1} to 6 m d^{-1} was calculated according to the difference in the hydraulic head between pumping well and a groundwater standpipe located behind the BHE. The resulting integral effective thermal conductivity of the whole BHE depth λ_{eff} was compared to the results of the GRTs at natural groundwater flow velocities of about 0 m d^{-1}. Maximum variations of λ_{eff} of about 10 % were obtained. The shape of the lowered groundwater level with its different flow velocities was neglected. Exact knowledge of the flow velocities, singular flow paths and the increase of $\lambda_{eff}(z)$ depending on the groundwater flow is not available.

Therefore, EGRTs were performed under natural and two different forced groundwater flows by the TUD in combination with the Groundwater Flow Visualization (GFV) measurement technique with resulting groundwater flow velocities over borehole depth $v_f(z)$. $\lambda_{eff}(z)$ were correlated with the determined groundwater flow velocities $v_f(z)$. The ratio of conductive and convective energy transport to the whole transported heat energy was evaluated.

SITE DESCRIPTION

The project area is located in Strausberg 40 km east of Berlin. On site, the energy demand of an office building is supported by 4 borehole heat exchangers (BHE). The depth of the BHE is 50 m each while the shape differs between single-U, double-U and coaxial pipes (Fig. 2).

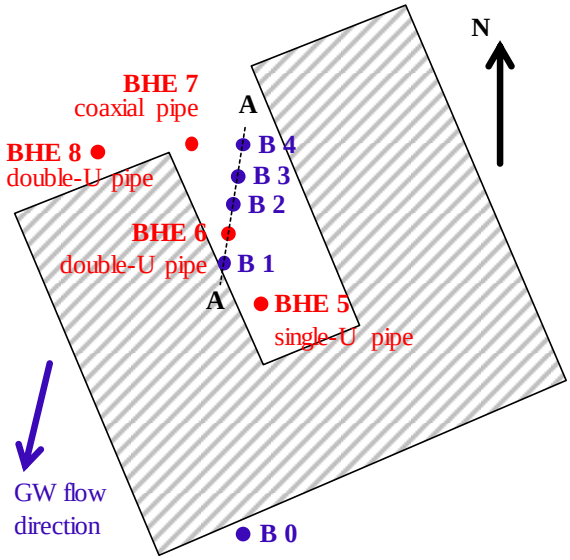

Figure 2. Location of the BHE and the standpipes

In preliminary investigations, the groundwater flow direction on site was determined with the aid of hydrogeological maps as well as with GFV measurement technique at an existing groundwater standpipe B 0 (31 m depth; 25 m south-west to BHE 6). The groundwater direction is pointing south-west (Fig. 2).

According to the groundwater flow direction 4 groundwater standpipes (B 1 – B 4) were drilled to varying depths of 31 m (B 0) – 37 m (B 4) and in distances 1.7 m (B 1) up to 7.9 m (B 0) to BHE 6 (Fig. 3). The filter pipes are located in the last 3 m (B 1 – B 3) respectively the last 6 m (B 4) of the borehole length.

The geological conditions on site can be summarized as follows: Covered by 6 m of gravely sandy fillings, an impermeable marl layer was investigated up to a depth of 21 m below ground. The marl is followed by a 4 m layer of coaly sand covering a loose sandy gravel layer up to the maximum drilling depth of 50 m. The loose sandy gravel package is only interrupted by a thin layer of marl in a depth of about 46.20 m – 47.50 m below ground.

Confined groundwater was encountered in all groundwater standpipes with an energy level of about 10.8 m below ground. The measured natural hydraulic gradient i between B 1 and B 2 is 0.007.

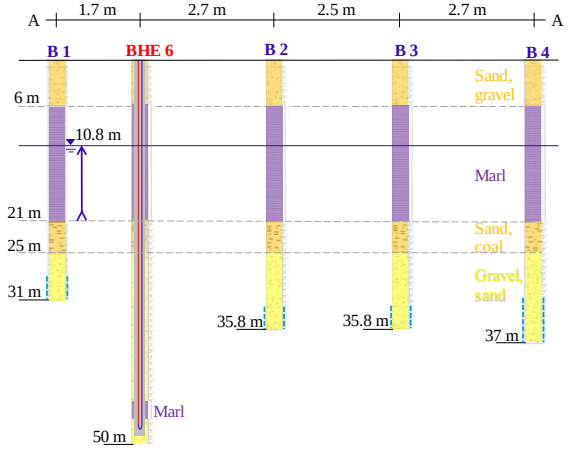

Figure 3. Geological section A-A

PERFORMED FIELD TESTS

Pumping tests

Two long-term pumping tests were performed on site. The duration of the tests was 5 days, each. Water was continuously extracted from B 4 with 3.4 $m^3 h^{-1}$ (Pumping Test 1) and 7.5 $m^3 h^{-1}$ (Pumping Test 2), while the groundwater level of the groundwater standpipes B 1 – B 4 was measured. The extracted groundwater was transported to an infiltration area about 70 m north-west of B 4.

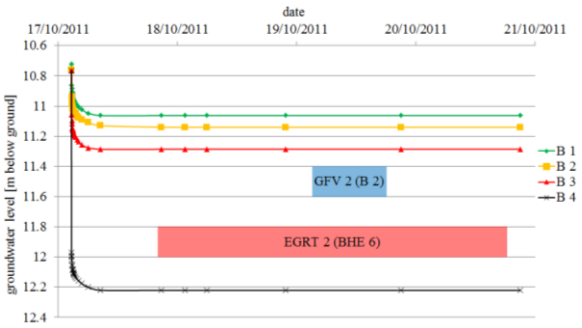

Figure 4. Results of Pumping Test 1 (3.4 $m^3 h^{-1}$)

A steady state was already reached within 1 day after the beginning of Pumping Test 1 caused by the fact that only the energy level of the confined groundwater was lowered (Fig. 4). Due to the pumping rate of 3.4 $m^3 h^{-1}$, the energy level of the groundwater standpipes was reduced from 10.8 m below ground to 11.1 m below ground (B 1) and 12.2 m below ground (B 4). The hydraulic gradient between B 1 and B 2 (at BHE 6) was determined to 0.016 (Pumping Test 1) respectively 0.029 (Pumping Test 2). The Darcy permeability k_f of the aquifer was determined to $3 \div 5 \cdot 10^{-4}$ m s^{-1}.

Due to the confined groundwater and the thin layer of marl in a depth of about 46.20 m – 47.50 m below ground, an almost horizontal groundwater flow can be assumed for BHE 6 in the depth of 21.0 m – 46.2 m (≈ 50 % of the whole length of the BHE) due to the pumping rates (Fig. 5).

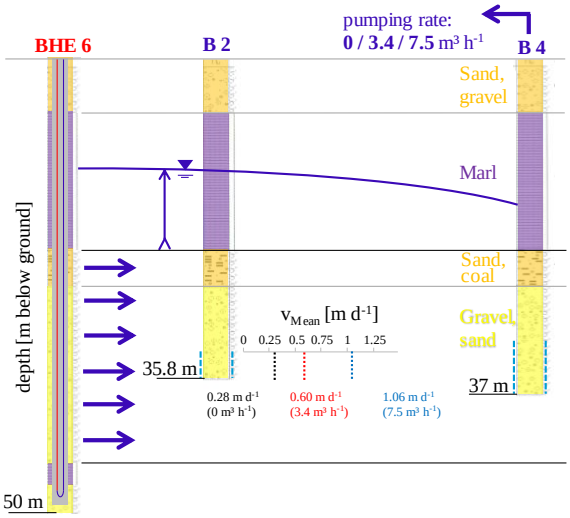

Figure 5. Horizontal groundwater flow while pumping test

GFV measurements

Three Groundwater Flow Visualization (GFV) measurements were performed at B 2. During a GFV measurement, a high resolution camera is located between two packers inside the filter pipe of a given groundwater standpipe. The camera recognizes suspended sediments transported by the groundwater and therefore, determines the groundwater flow direction and velocity. Extensive information on the theoretical background of the GFV measurement is given in (Schöttler, 1997).

While GFV 1 evaluated the natural groundwater flow velocity and direction, GFV 2 and GFV 3 were performed at the steady state of Pumping Test 1 (GFV 2) and Pumping Test 2 (GFV 3) (Fig. 4).

The results of GFV 1 – GFV 3 performed in the filter pipe of B 2 (34.0 – 35.8 m) can be summarized as follows: The natural groundwater flow direction determined in GFV 1 (175°) is in good agreement with the groundwater flow direction according to hydrogeological maps (Fig. 2). The natural groundwater velocity varies between 0.09 m d^{-1} and 0.51 m d^{-1} with a weighted mean according to the quality of every single measurement of 0.28 m d^{-1}.

The groundwater flow direction determined in GFV 2 and GFV 3 differs from the natural groundwater flow direction for in almost 180° (Fig. 6). The weighted mean of the groundwater flow directions is about to the north (349°), in direction of pumping well B 2.

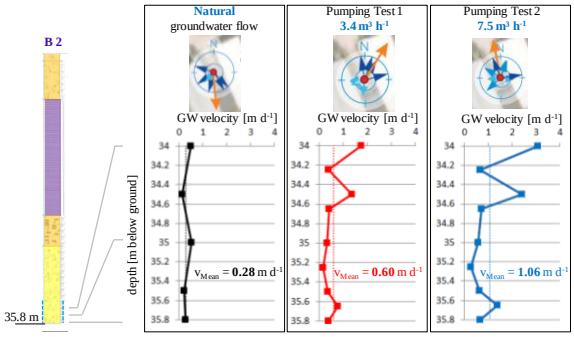

Figure 6. GFV measurement

According to the pumping rates the groundwater flow velocities increases in GFV 2 (3.4 $m^3 h^{-1}$) to 0.15 m d^{-1} – 1.75 m d^{-1} (weighted mean = 0.6 m d^{-1}) and in GFV 3 (7.5 m^3 h^{-1}) to 0.24 m d^{-1} - 3.09 m d^{-1} (weighted mean = 1.06 m d^{-1}).

Enhanced Geothermal Response Test

Three Enhanced Geothermal Response Tests (EGRT) were performed at BHE 6 in July (EGRT 1), October (EGRT 2) and November (EGRT 3) 2011. Instead of using the copper cable of the installed hybrid cable the thermal load was fed on BHE 6 with the help of a Geothermal Response Test (GRT) device. Therefore, the results of the EGRTs can be validated by the results of the common GRTs. The GRT device was connected to one of the double-U pipes and a constant thermal load of 2617 W / 52.3 W m^{-1} (EGRT 1), 2302 W / 46.0 W m^{-1} (EGRT 2) and 2075 W / 41.5 W m^{-1} (EGRT 3) was applied for 62 h (EGRT 1) respectively 70 h (EGRT 2, EGRT 3).

While EGRT 1 was performed without any groundwater extraction, EGRT 2 was carried out at the steady state of Pumping Test 1 with a pumping rate of 3.4 $m^3 h^{-1}$ (Fig. 4) and EGRT 3 was carried out at the steady state of Pumping Test 2 with a pumping rate of 7.5 $m^3 h^{-1}$ (EGRT 3).

The undisturbed temperature profile over the borehole depth at the start of the heating phase varies from 11.7°C to 15.6°C (Fig. 7). By neglecting the first 6 m below ground, which is strongly influenced by atmospheric temperature variation, the geothermal gradient was determined to be at 0.03 K m^{-1}. The temperature profile 60 h after starting the heating phase, varies from 19.9°C to 23.6°C.

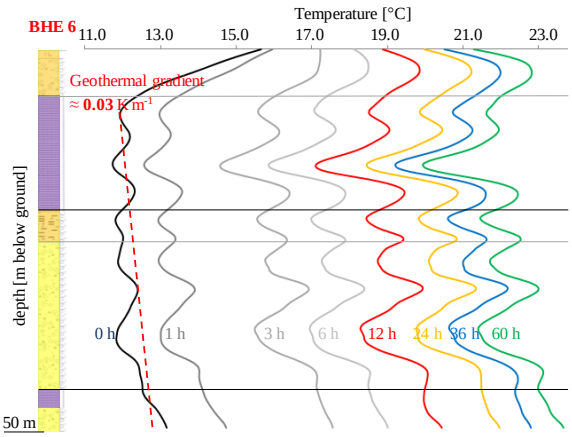

Figure 7: Temperature profiles over depth (EGRT 1)

The temperature development over time increases in different depths according to the geological and hydrogeological conditions from the undisturbed temperature profile with different slopes up to 20.0°C (15 m / marl), 22.2°C (23 m / sand, coal), 21.9°C (36.5 m / gravel, sand) and 23.5°C (31.5 m / gravel, sand) (Fig. 8). The increase of temperature k is inversely proportional to the effective thermal conductivity $\lambda_{eff}(z)$. Neglecting borehole resistivity and other effects the effective thermal conductivity of water saturated systems is primarily the sum of conduction and convection. A low increase of the temperature is therefore caused by a high thermal conductivity of the ground or a high groundwater flow.

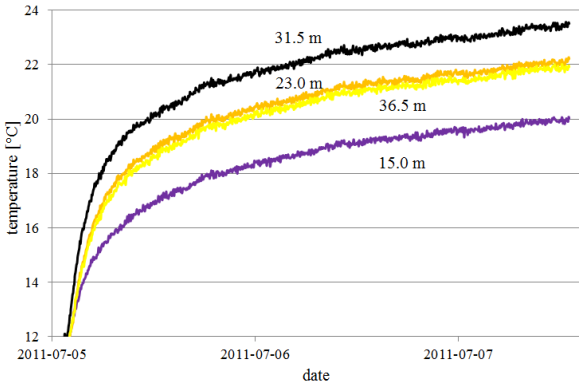

Figure 8: Temperature development over time (EGRT 1)

According to the slope k of the temperature development, the effective thermal conductivity over depth $\lambda_{eff}(z)$ can be determined by the Source Theory (Fig. 9). The determined mean effective thermal conductivity $\lambda_{eff}(z = 0 - 50m)$ increases according to the applied groundwater flow velocities from 2.11 W m^{-1} K^{-1} (EGRT 1) to 2.37 W m^{-1} K^{-1}

(EGRT 2) and 2.49 W m^{-1} K^{-1} (EGRT 3). That means an increase of 12.3 % respectively 18.0 %.

Especially in the gravely, sandy aquifer layer (21 m – 46.2 m), where groundwater flow occurs, a high increase of the effective thermal conductivity $\lambda_{eff}(z = 21 - 46.2m)$ of 13.3 % (EGRT 2) and 21.9 % (EGRT 3) can be observed. According to singular flow paths in the aquifer an increase of the effective thermal conductivity $\lambda_{eff}(z = 34m)$ in chosen incremental depths of even 16.6 % (EGRT 2) and 32.2 % (EGRT 3) can be determined (Table 1).

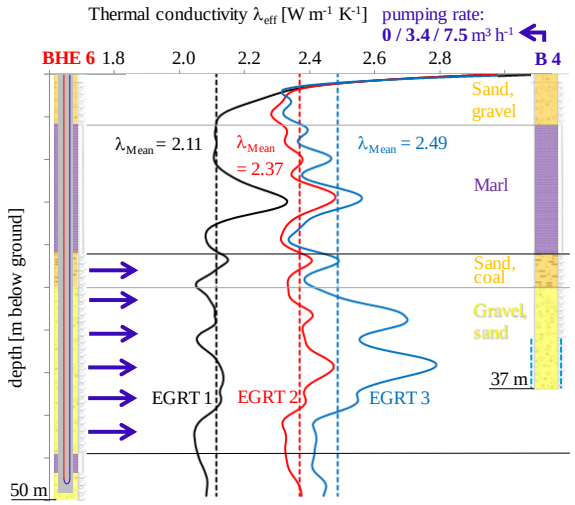

Figure 9: Effective thermal conductivity over depth (EGRT 1, EGRT 2, EGRT 3)

The evaluated effective thermal conductivities for the sections 0 m - 50 m, 21 m - 46.2 m and 34 m are summarized in Table 1.

Table 1: Determined eff. thermal conductivity and its increase for different sections

section	eff. thermal conductivity [W m^{-1} K^{-1}]		
	EGRT 1	EGRT 2	EGRT 3
0 – 50 m	2.11 (ref.)	2.37 (+12.3 %)	2.49 (+18.0 %)
21 – 46.2 m	2.1 (ref.)	2.38 (+13.3 %)	2.56 (+21.9 %)
34 m	2.11 (ref.)	2.46 (+16.6 %)	2.79 (+32.2 %)

CONCLUSIONS

After all, 3 EGRTs under natural and artificial increased groundwater flows were performed from July – November 2011. By the means of the Groundwater Flow Visualization measurement technique the effective groundwater flow velocities over depth were determined and compared to the effective thermal conductivities. An increase of the effective thermal conductivity up to 32.2 % according to the increased groundwater flow velocity was evaluated. Currently all the results are compared to the performed laboratory tests and reanalyzed with numerical methods.

REFERENCES

Glück, B. (2008), "Simulationsmodell „Erdwärmesonden" zur wärmetechnischen Beurteilung von Wärmequellen, Wärmesenken und Wärme-/Kältespeichern". Rud. Otto Meyer-Umwelt-Stiftung, Hamburg, 2008.

Hartog, A. H. and D. N. Payne (1982), „A fibre-optic temperature-distribution sensor", IEE Colloqium Optic Fibre Sensors.

Hurtig, E., J. Schrötter, S. Großwig, K. Kühn, B. Harjes, W. Wieferig and R. P. Orrell (1993), „Borehole temperature measurements using distributed fibre optic sensing", Scientific Drilling, 3: 283–286.

Katsura, T., Nagano, K., Hori, S., Okawada, T. (2009), "Investigation of groundwater flow effect on the thermal response test result". Proceedings of 11th Energy Conservation Thermal Energy Storage Conference. Stockholm. 15.-17. June 2009.

Kleiner, S. (2003), „Untersuchungen zur Optimierung von Erdwärmesondenanlagen - petrophysikalische Messungen und numerische Simulationen".

Pannike, S., Kölling, M., Panteleit, B., Reichling, J. (2006), "Auswirkung hydrogeologischer Kenngrößen auf die Kältefahnen von Erdwärmesondenanlagen in Lockersedimenten", Grundwasser – Zeitschrift der Fachsektion Hydrogeologie 1/2006.

Schöttler, M. (1997), „Meßbarkeit der Grundwasserbewegung durch Visualisierung der Strömung in Bohrbrunnen", Aachen.

Spitler, J. D., Simon, J. R., Chiasson, A.D. (1999), "Incorporation of groundwater flow into numerical models and design models", Oklahoma State University.

Witte, H. J. L. and van Gelder A. J. (2006), "Geothermal Response Tests using controlled multi-power level heating and cooling pulses (MPL-HCP): quantifying ground water effects on heat transport around a borehole heat exchanger", Proceedings of Ecostock, The Tenth International Conference on Thermal Energy Storage, Richard Stockton College, New Jersey, U.S.A.